*12th IMEKO TC4 International Symposium*
*Electrical Measurements and Instrumentation*
*September 25–27, 2002, Zagreb, Croatia*

# VOLUMETRIC CAROTID PLAQUE MEASUREMENTS BASED ON ULTRASOUND IMAGES: A PRELIMINARY APPROACH

*D. Capriglione(1), L. Ferrigno(1), C. Liguori(1), A. Paolillo(2)*

(1) DAEIMI University of Cassino, via G. Di Biasio, 47, Cassino (FR) – Italy- e_mail: liguori@unicas.it
(2) DIIIE University of Salerno, via Ponte Don Melillo, Fisciano (SA) - Italy e_mail: apaolillo@unisa.it

**Abstract –** In the paper a measurement system for the carotid occlusion volume, based on 3-D ultrasound imaging is proposed. The system has been designed taking into account two main tasks: computational effort and measurement accuracy. The analysis of the uncertainty of the whole measurement chain and first experimental results on carotid images are given.

Keywords: 3-D imaging, ultrasound image, volume measurements, carotid artery.

## 1. INTRODUCTION

The arteriosclerosis processes are strongly correlated to the presence of thickening and plaques in carotid. Non-invasive methods, as ultrasound techniques (B-mode, color Doppler, Color Power Angio, here in after CPA) can clearly detect these phenomena. In fact, the analysis of the obtained images allows to find out a plaque and to evaluate its nature and shape. The most clinical ultrasound tests are based on 2-D image analysis thanks to its simplicity and promptness. But with this kind of test some 3-D information, in particular about the carotid occlusion volume, could be lost. The diagnostician can make some qualitative 3-D reconstruction, but it strongly depends on the experience and the knowledge of the operator. Consequently, there is a growing clinical interest in 3-D ultrasound imaging, since 3-D visualization of the carotid artery can help in the accurate definition of the size and three-dimensional features of arteriosclerosis plaques [1], [2].
As an example, in [3] a system for the classification of artery plaques is presented. It is based on a reconstruction of the carotid features starting from five images, scanned from different angles. The images are processed to build a set of five volume images, then on these volumes some features are extracted. The extracted features will be used in order to identify calcification and fibrous tissues in the artery. In [4] a semi-automated method for segmenting 3-D ultrasound images is described; the segmentation algorithm seems to be very performing but no information are given on the 3-D reconstruction. In [5] a linear phased probe array for the acquisition of dimensionally 3-D ultrasound data from multiple 2-D image planes is proposed. The reported results indicate that the obtained accuracy on the image reconstruction is suitable for clinical requirements, but no algorithm for feature extraction is presented.
The authors are working in this framework [6], and, in particular, they are designing and realizing an ultrasound imaging systems for high accuracy carotid plaque volume measurement. Preliminary studies were carried out in order to investigate on well-suited hardware and software solutions highlighting the connected problems. On the basis of these preliminary studies, a measurement 3-D prototypal system was set-up. In particular the proposed system is able to: (*i*) reconstruct the image of the carotid artery, (*ii*) evaluate the plaque volume, (*iii*) calculate the percentage of carotid occlusion.
In the following, at first the realized prototype will be described in detail highlighting the features and the current limits of the adopted solutions, furthermore preliminary experimental results on simulated arteries and on real carotid images will be illustrated.

## 2. THE REALIZED PROTOTYPE

A typical measurement system based on 3-D ultrasound imaging [7] can be schematized as reported in Fig. 1. The first stage is composed by necessary hardware to capture the 2-D images. The acquired two-dimensional images are processed in order to extract some information required for the 3-D reconstruction. Finally the 3-D image is processed to achieve the required measurements. Generally the 3-D reconstruction can be realized in two distinct ways:

- Each 2-D image is segmented, in the current plane, to extract the object contours, which are used to obtain the object surface;
- Defining a voxel as the elementary component in a 3-D space, a voxel-based image is built by placing each pixel in its correct position in the 3-D space. The gray-level of any not sampled voxel is calculated by an interpolation algorithm [3], [7].

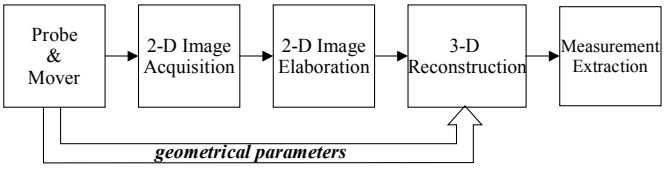


Fig. 1. Block diagram of a measurement system based on 3-D ultrasound imaging

The advantage of the first approach is the reduction in the amount of data, because only the interesting points are processed; consequently a more efficient 3-D rendering is achieved, whereas on the other hand some information could be lost in the segmentation phase. Vice-versa the voxel-based approach is more time consuming and resource demanding, but, no information is lost [7].
Taking into account these preliminary considerations, the first approach was chosen for the realized prototype.
In the following the blocks composing the prototypal measurement system are described in detail.

### *2.1 The probe and mover*

A basic point in the realization of the whole prototype is the right choice of the ultrasound probe and the mover system. A good quality in the acquired images and accurate information on the probe position are necessary to obtain correct edge detection and accurate 3D reconstruction, respectively. For these reasons CPA imaging techniques have been selected; they highlight also slow blood fluxes to be evidenced whichever the ultrasound orientation could be with respect to the flux direction. The used probe is an ATL 5000 by Philips, with 7-12MHz changeable pulse ultrasound frequency. In particular, 10MHz frequency was chosen, since it allows up to 39 mm analysis depth with a good resolution. Consequently, a very wide variety of carotid arteries can be analyzed (generally the carotid is modeled like a tube with a medium circular section of about 1 cm of radius and with the center placed under the skin at 12-20 mm depth). As an early step, a freehand scanning prototype was realized. The insonification angle, namely the angle between the start analysis plane and current scanning plane, was evaluated by applying a probe package, which was provided with a goniometer. This prototypal realization allowed the first experimental tests to be done with acceptable precision.

### *2.2 2-D image acquisition*

A suitable set of 2-D CPA carotid images was acquired in order to find out the optimal arrangement in terms of patient position, 2-D type images and acquiring set-up to allow the best 3-D reconstruction and reliability to be achieved. In particular, in this phase some aspects should be separately considered:

- Type of image to acquire for 3-D reconstruction;
- Choice of scanning angles;
- Number of images to acquire;
- Timing in the image acquisition;
- Patient arrangement.

As for the 3-D reconstruction different solutions could be adopted such as to use transversal images (Fig. 2a), longitudinal images (Fig. 2b) or mixed solutions. Many experimental tests were carried out and they proved that the optimal choice in terms of image quality and 3-D reconstruction is achieved using longitudinal images; moreover the best longitudinal images are obtained by placing the probe in a back-lateral position.
As far as the scanning angles are concerned, the wider the scanning angle, the more detailed the reconstruction but the less clear the obtained image. Consequently the maximum scanning angle is experimentally determined taking into account the tradeoff among reconstruction accuracy and image sharpness.

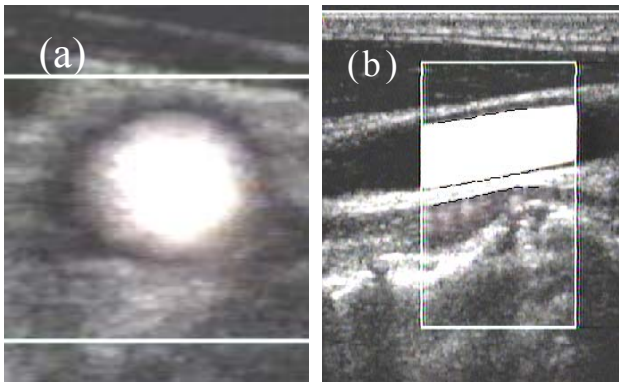


Fig. 2. Carotid artery transversal (a) and longitudinal (b)view

More in detail, the technician looks for the probe position which allows the maximum diameter of the carotid in the display; then, he slowly tilts the probe until a clear still image is acquired. A total scanning angle of 10 degrees, ±5 degrees from the best position (zero insonification angle) was evaluated. As an example Fig. 3 shows three images acquired at –5°, 0, +5° insonification angles.
As for the minimum number of 2-D scans necessary for an acceptable accuracy in the 3-D reconstruction, a simulation environment was used, as detailed in section 4. In particular, many tests were carried out changing the number of slices extracted by the emulated artery. It was determined that the error in the volume measurement due to the sampling becomes negligible with respect to accuracy required in medical application using a minimum number of ten sections (one degree insonification angle step). In this first realization, however, it was not possible acquire ten images because of the limited resolution of the adopted mover; consequently only five images were acquired and processed.
As for timing in the image acquisition, some considerations have to be made about the synchronization between the image acquisition process and the movement of the cardiac muscle. The blood flows in the carotid pumped by the cardiac muscle, therefore the carotid expands and contracts itself following the same rhythm of the heart. Consequently, it is necessary to acquire all scans with the carotid in the same conditions, otherwise an uncorrected reconstruction and a wrong volume measurement is obtained. To this aim a built-in electrocardiograph (ECG) provides a trigger for the image acquisitions. In particular, the CPA ultrasound images are sampled with a time delay of a half heart period after the systolic instant. As far as the patient arrangement is concerned, a further error source could be due to possible

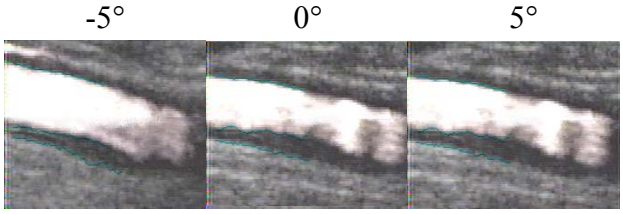


Fig. 3. Images of the same artery acquired with different angles

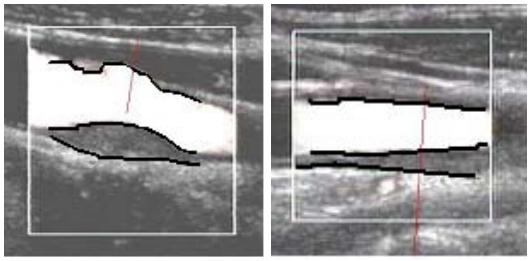

Fig. 4. Some results of the segmentation procedure

movements of the patient, like the respiratory ones. Therefore, the carotid image acquisition is performed asking the patient to hold his breath.

Summarizing, the procedure for the 2-D image acquisitions is the following:

- The probe is suitably positioned on the patient neck;
- The operator handles the probe until both best longitudinal view and image quality are reached;
- The operator captures the image, and selects a box for the CPA modality;
- The probe is rotated around the pivot axis until another defined angular position is reached;
- The previous steps are repeated until the chosen number of acquisition is completed (the deviation is constrained in ±5 degrees).

### *2.3 2-D image processing*

Each 2-D image is processed in order to extract the three interfaces: intima-lumen in near wall, intima-lumen in far wall, lumen-plaque. The segmentation is completely automatic [6]. The technician is required only to select the region of interest (ROI) for the image analysis, aiming to simplify the elaboration software and to reduce the elaboration time. The contour detection algorithm is specific for CPA images and employs a dynamic programming procedure [8]. This method is based on the recursive application of suitable *cost functions*. Namely, three cost functions are used, one for each interface. They are constituted by some terms taking into account the characteristics of the investigated contours: as an example, gray level above and below the contour; the contour regularity. These terms are weighted by coefficients empirically evaluated during a training phase performed on different carotid CPA images. In Fig. 4 the results of the segmentation procedure for two CPA images are shown.

### *2.4 3-D reconstruction*

In this phase the extracted contours are combined to obtain the artery surface. Each pixel composing the segmented artery interface is transposed from the 2-D scanning plane (x', z') into 3-D Cartesian system (x, y, z), obtaining the 3-D artery surface; to this aim, the following relationships were used:

$$\begin{bmatrix} x \\ y \\ z \end{bmatrix} = \begin{bmatrix} 1 & 0 \\ 0 & \sin(\theta_i) \\ 0 & \cos(\theta_i) \end{bmatrix} \cdot \begin{bmatrix} x' \\ z' \end{bmatrix} \quad (1),$$

where $\theta_i$ are the insonification angles. The above mentioned reconstruction process is illustrated in Fig. 5, in particular fig. 5 (a) shows the interfaces related to a single 2-D image, while in fig 5 (b) the positioning of the interface pixels of 2-D images corresponding to other insonification angles is reported.

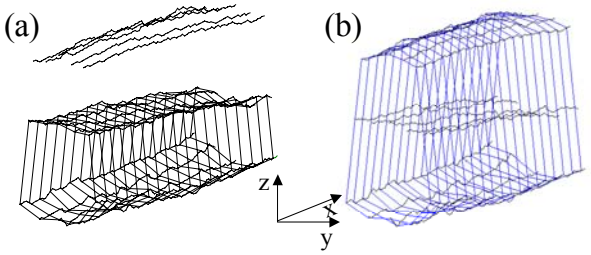


Fig. 6. The reconstructed 3-D interfaces (a) plaque volume, (b) lumen volume

### *2.5 Measurement extraction*

The plaque volume evaluation is carried out considering cross sections of the reconstructed 3-D surface.

The 3-D object is sliced in the *x* direction, with a x-step, Δx, equal to a pixel. For each cross section in the *z-y* plane the area, $A_p$, delimited by the interpolated lumen-plaque and far wall lumen-intima interfaces Fig. 6 (a) is evaluated. The area of the so obtained polygon is computed by dividing it into adjacent triangles with consecutive points of the section contour (Fig. 7). The following relationship is used:

$$A_P = \frac{1}{2} \cdot \left| \sum_{i=1}^{M} (y_i \cdot z_{i+1} - y_{i+1} \cdot z_i) \right| \quad (2)$$

where M is the number of polygon vertices, and the M+1$^{th}$ point coincides with the first $(y_{M+1}, z_{M+1})=(y_1, z_1)$; it has to be noted that M/2 is equal to the number of acquired images. The evaluation of single slice volume is achieved by

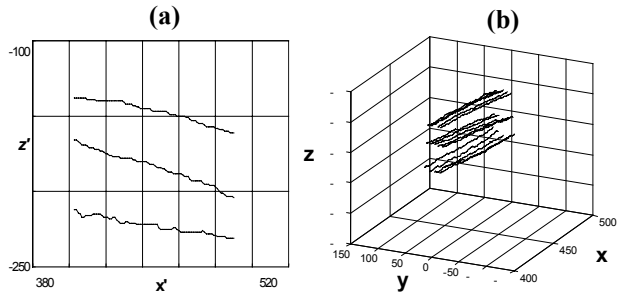


Fig. 5. The contour lines positioning procedure

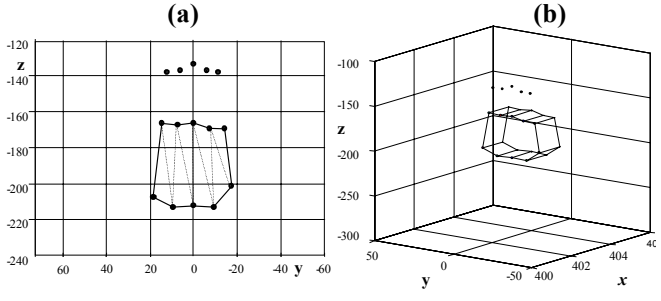


Fig. 7. An example of (a) area and (b) single slice volume evaluation

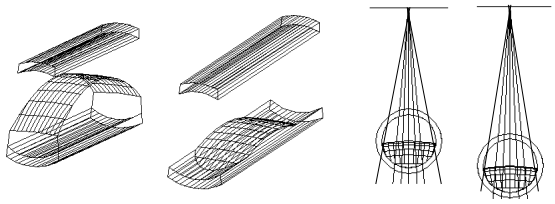

Fig. 8. The emulated artery with plaques

multiplying the cross sectional area $A_P$ and the x-step, $\Delta x$. Finally the plaque volume is obtained summing the single slice volumes:

$$V_P = \sum_j A_{Pj} \Delta x \quad (3)$$

The achieved measurement values are expressed in pixel (pixel$^2$, pixel$^3$); in order to obtain the corresponding values in mm (mm$^2$, mm$^3$) a system calibration is needed. Since the proposed prototype works with a fixed frequency, the calibration [6] was carried out only once. A pixel-millimeter conversion factor, k, equal to 0.08mm/pixel was determined. Consequently, the plaque volume in millimeter was evaluated as:

$$V_p^{mm} = k^3 V_p \quad (4)$$

The volume of lumen, $V_L$ is evaluated in the same way, but considering the intima-lumen interfaces (in the near and far wall), Fig. 6 (b).
A more helpful parameter, the occlusion percentage, $O_{\%}$, is determined; it is obtained as the ratio between the plaque and the lumen volumes:

$$O_{\%} = \frac{V_P}{V_L} \cdot 100 \quad (5)$$

## 3. TUNING OF THE PROTOTYPE

Once the proposed prototype has been realized, a tuning phase is required in order to evaluate the optimal parameter choices and system performances. This adjustment phase is based on a preliminary simulation analysis followed by experimental validation tests.

### *3.1 2-D image processing*

In order to evaluate the performances of segmentation 2-D image algorithm, and to determine the accuracy in the identified interfaces a set of experimental tests were carried out. It includes a suitable variety of images characterized by different features in terms of edge contrast, sharpness, noisy and geometrical plaque characteristics.
At first, the repeatability in the edge location was evaluated. In particular, for each acquired image, N=30 images are generated adding impulsive noise to it. On these new image sets, the segmentation algorithm is run and for each *x'* pixel coordinate, the variability of the extracted contour *z'* was evaluated. With reference to common quality images a repeatability of 100% was measured, while a 90% was observed for poor quality images .

Then, the reliability of the procedure was evaluated comparing the localized edges with the ones achieved by a human technician. A very good agreement was observed. The correlation factor between the automatic and manual edge ordinates was never less than 0.98, and the distance among the two *z'* was always constrained in 5 pixels.

### *3.1 3-D reconstruction and measurement extraction*

In order to verify the performance of the measurement extraction phase, the software prototype was tested on artificial images reproducing the human carotid, obtained in a 3D CAD environment (Autocad 2000).
The artery is reproduced like a cylinder and a plaque with spherical shape is positioned inside it. Several plaques of different sizes were simulated and different positions of the carotid respect to the skin were considered (see Fig. 8). It has to be noted that in this way the lumen and the plaque volume are well-known, since they are built in a simulation environment.
The 2-D acquisition process is emulated slicing the simulate artery: for each insonification angle a corresponding plane is built; the volume sections projected in the selected planes give the 2-D images. As said in section 3.2, five planes rotating in the interval [-5°,+5°] around pivot axis, were considered.
The prototype software processes the obtained artificial 2-D images in order to reconstruct the plaque and to evaluate the measurements. Following this approach the error of the measurement system on the carotid plaque volume is calculated; the connected results are summarized in Tab. I. A systematic effect is highlighted: the measurement error is negative for each test (the system underestimate the volume). This effect is due to the poor number of acquisitions, taken at five different insonification angles instead of ten, and can be corrected as:

$$V_p^c = c \cdot V_p^{mm} = c \cdot k^3 V_p \quad (6)$$

where $c = 1 - \frac{e\%}{100}$ is the correction factor.

Some considerations have to be made about the value used for the correction factor. As shown in Tab. I, the percentage error value depends on both carotid position and plaque dimension; consequently the correction factor *c* should assume different values according with these parameters. Referring to Tab.I, it is possible to observe that the percent error variation is contained in a 1% range. Consequently, taking into account all uncertainty sources present in the realized prototype these variations can be considered negligible. For this reason, a *c* mean value is used (c=1.032), and the corresponding measurement uncertainty was

TABLE I. The errors in plaque volume measurements
(d=carotid-probe distance)

| Actual | d=12 mm | | d=15 mm | | d=18mm | | d=21 mm | |
|---|---|---|---|---|---|---|---|---|
| Value | Vmis | e % | Vmis | e % | Vmis | e % | Vmis | e % |
| 117.00 | 113.73 | -2.88 | 113.95 | -2.68 | 113.63 | -2.97 | 113.39 | -3.18 |
| 100.00 | 97.85 | -2.20 | 97.25 | -2.83 | 96.97 | -3.12 | 96.61 | -3.51 |
| 83.00 | 81.02 | -2.44 | 80.56 | -3.03 | 80.33 | -3.32 | 80.04 | -3.70 |
| 66.00 | 64.05 | -3.04 | 63.95 | -3.20 | 63.89 | -3.30 | 63.36 | -4.17 |
| 50.00 | 48.12 | -3.91 | 48.38 | -3.35 | 48.26 | -3.61 | 48.08 | -4.00 |
| 35.00 | 34.20 | -2.34 | 33.89 | -3.27 | 33.81 | -3.53 | 33.97 | -3.04 |

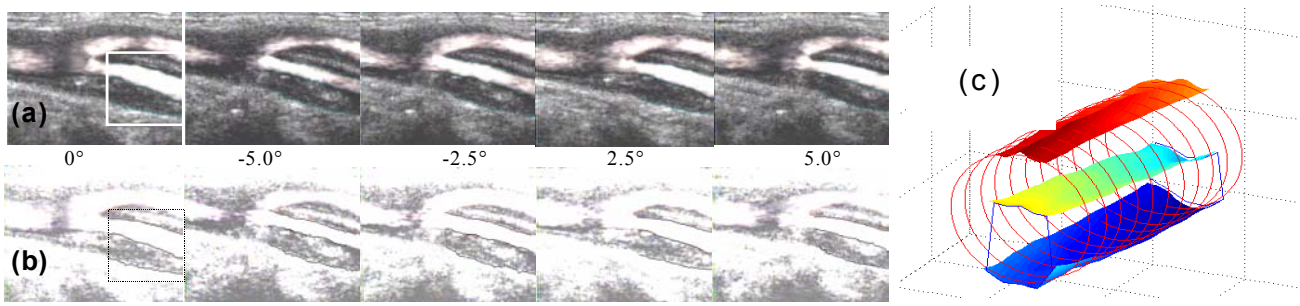


**(d)** $V_P$=37(2) mm$^3$; $V_L$=160(8) mm$^3$;$O_{\%}$=23(1)%.

Fig. 9. The provided results the carotid **A**. (a) the five acquired images; (b) the segmented contours; (c) the reconstructed 3D artery; (d) the measured values with their standard uncertainty in parenthesis.

considered equal to the measured standard deviation ($U_c$ = 0.005).

The same procedure was adopted also to estimate the correction factor in the carotid volume measurement: the mean and deviation values turned out are the same with good approximation.

## 4. EXPERIMENTAL RESULTS

After the tuning phase some experimental results were conducted on patients affected by carotid stenos. For sake of brevity only four tests are reported in this section. The major medical attentions are directed in examinations of the presence of plaques near or within the internal carotid; this is the most frequent and dangerous case. For this reason the reported cases regard the presence of plaques near the bifurcation (example **A**), in the internal carotid (examples **B**, **C**) and in the common carotid (example **D**).

TABLE II. Synthesis of the results obtained for carotids **B**, **C** and **D**

**B**

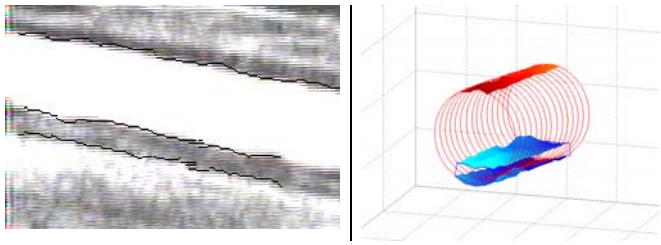

$V_P$=37(2) mm$^3$; $V_L$=160(8) mm$^3$;$O_{\%}$=23(1)%.

**C**

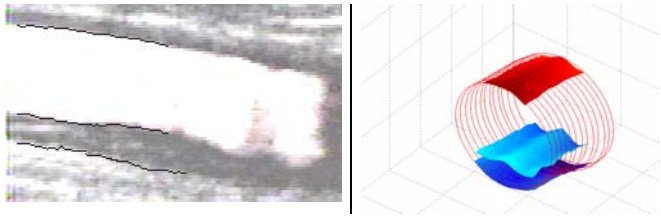

$V_P$=29(1) mm$^3$; $V_L$=144(6) mm$^3$; $O_{\%}$=20(1)%.

**D**

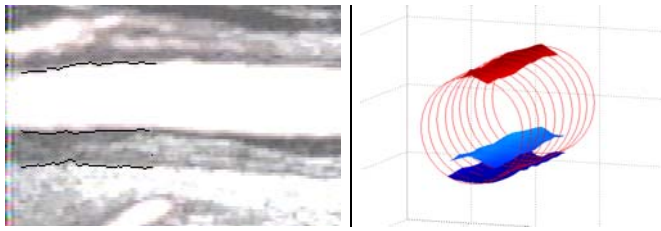

$V_P$=24(1) mm$^3$; $V_L$=96(3) mm$^3$; $O_{\%}$=25(1)%.

The operative conditions are the same described in section 2: 5 CPA longitudinal images were acquired in a +/- 5° range around the zero insonification angle, with a regular angle step of 2.5°.

Fig. 9 shows the results concerning the example **A**. In particular Fig. 9(a) shows the five acquired images; Fig.9(b) reports the results of the segmentation phase evidencing both the selected ROI and the goodness of the segmentation phase; Fig. 9(c) presents the 3-D reconstruction of the near wall, far wall and the plaque interfaces. The prototype indicates also the measured values of plaque, lumen volume and occlusion percentage with their standard uncertainty as reported in Fig. 9(d). The uncertainty of the results is evaluated by the prototype software, implementing the relationships reported in appendix. The results of successive experiments (**B**, **C**, **D**) are summarized in Tab. II that contains, for each case, the segmented zero angle insonification image, the 3D reconstruction and the measurements results.

On the basis of the obtained result some consideration can be made: the measurements uncertainty is constrained within 5% of the measurement value; the segmentation results are perfectly accorded with those expected by several expert technicians, and cardiologists.

## 5. CONCLUSIONS

The project and a first realization of a prototypal system able to measure the volume occlusion caused by the presence of plaques in the human carotid was presented in the paper. Novelties of the realized system, compared with the others present in literature, are: (i) the 3D reconstruction and the volume measurements are made on the segmented images and not on the gray scale full image, thus allowing the reduction of the elaborated data and the measurement time. (*ii*) The realized system uses CPA images that are less noisy respect to the traditional B-mode images and allow to find also anechoic plaques. (iii) Plaque dimensions are numerically evaluated with their uncertainty. First experimental results are well promising for the future implementation of the final automatic system. In fact, in spite of the reduced number of acquired images, the

obtained uncertainty seems to be interesting for medical purpose. Further improvements will concern the realization of an automatic scan system able to move the probe with an angular precision less than 0.1°.

ACKNOWLEDGMENT

The authors wish to thank Drs. Luigi Di Siena and Giuseppe Di Leo for their help in the experimental work, Dr. Pasquale Guarini and Prof. Antonio Pietrosanto for the suggestions in the prototype design and characterization.

## APPENDIX: METROLOGICAL CHARACTERIZATION OF THE MEASUREMENT ALGORITHM

Due to the carotid variability caused by the natural activity of the cardiac organ, and to the absence of a reference system, an experimental metrological characterization of the measurement cannot be carried out. For this reason an *a-priori* analytical evaluation of the measurement uncertainty [9], is performed. The uncertainty propagation law, suggested by the ISO-GUM [10] is applied at the relationships implemented in the prototype software.

As for the uncertainty on the plaque volume measurement, from eq. 6, we have:

$$U^2_{V_p^c} = \left(\frac{\partial V_p^c}{\partial c}\right)^2 U_c^2 + \left(\frac{\partial V_p^c}{\partial k}\right)^2 U_k^2 + \left(\frac{\partial V_p^c}{\partial V_P}\right)^2 U^2_{V_p} = \\ = V_p^c \cdot \left[\left(\frac{U_c}{c}\right)^2 + \left(\frac{U_k}{k}\right)^2 + \left(\frac{U_{Vp}}{V_P}\right)^2\right] \quad \text{(A1)}$$

where $U_c, U_k, U_{Vp}$ are the absolute standard uncertainty of c, k, $V_P$, respectively, and are evaluated as follow.

As for $U_c$, it is evaluated considering a standard deviation of the relative error measured on all tests, as described in section 4. Its estimated value is:

$$U_C = 0.005 \quad \text{(A2)}$$

As far as $U_k$ is concerned, we can pose, with a good approximation [7]:

$$U_k = 0.2 \cdot 10^{-3} \frac{\text{mm}}{\text{pixel}} \quad \text{(A3)}$$

The uncertainty on $V_p$, is evaluated by eq. 3, considering the areas of each cross section, $A_{pj}$, uncorrelated and $\Delta x$ equal to one pixel and consequently without uncertainty:

$$U^2_{V_p} = \sum_j \left(\frac{\partial V_p}{\partial Aj}\right)^2 U^2_{Aj} = \sum_j \Delta x^2 U^2_{Aj} \quad \text{(A4)}$$

In order to evaluate the $j^{th}$ cross section area uncertainty, the ISO-GUM law is applied to eq. 2, assuming uncorrelated the 3-D coordinates of the plaque contour pixels:

$$U^2_{Aj} = \sum_{i=1}^{M} \left(\frac{\partial Aj}{\partial y_i}\right)^2 U^2_{y_i} + \left(\frac{\partial Aj}{\partial z_i}\right)^2 U^2_{z_i} + 2\frac{\partial Aj}{\partial y_i}\cdot\frac{\partial Aj}{\partial z_i} U(y_i, z_i) \quad \text{(A5)}$$

Analyzing each component:

$$\frac{\partial Aj}{\partial y_i} = z_{i+1} - z_{i-1}; \frac{\partial Aj}{\partial z_i} = y_{i+1} - y_{i-1}, \text{for } i = 1..M \quad \text{(A6)}$$

In order to evaluate the uncertainty on the 3-D coordinates eq. 1 is considered, achieving:

$$U^2_y = \left(\frac{\partial y}{\partial z'}\right)^2 U^2_{z'} + \left(\frac{\partial y}{\partial \theta}\right)^2 U^2_\theta = \sin^2(\theta) U^2_{z'} + (z')^2 \cos^2(\theta) U^2_\theta \quad \text{(A7)}$$

$$U^2_z = \left(\frac{\partial z}{\partial z'}\right)^2 U^2_{z'} + \left(\frac{\partial z}{\partial \theta}\right)^2 U^2_\theta = cos^2(\theta) U^2_{z'} + (z')^2 sin^2(\theta) U^2_\theta$$

$$U(y,z) = \frac{\partial y}{\partial z'}\cdot\frac{\partial z}{\partial z'} U^2_{z'} + \frac{\partial y}{\partial \theta}\cdot\frac{\partial z}{\partial \theta} U^2_\theta = \\ = \sin(\theta)\cos(\theta) U^2_{z'} - (z')^2 \sin(\theta)\cos(\theta) U^2_\theta \quad \text{(A8)}$$

The uncertainty on the edge position $U_{z'}$ depends on the image noise, the edge detection algorithm and so on [14]; it was experimentally evaluated: $U_{z'} = \frac{5}{\sqrt{3}}$.

The uncertainty on the insonification angle depends on the resolution of the package used to evaluate the angles. Since angle resolution was 0.1°, assuming a rectangular distribution we have: $U_\theta = \frac{0.1°}{\sqrt{3}}$ (A9)

The same steps are made for the estimation of lumen volume uncertainty.

In the evaluation of the occlusion percentage the conversion and correction factors do not contribute to the uncertainty:

$$U^2_O = \left(\frac{\partial O}{\partial Vp}\right)^2 U^2_{Vp} + \left(\frac{\partial O}{\partial V_L}\right)^2 U^2_{V_L} = O\cdot\left(\frac{U^2_{Vp}}{V^2_P} + \frac{U^2_{V_L}}{V^2_L}\right) \quad \text{(A10)}$$

## REFERENCES

[1] K. Rosenfield, et alii, "Three-dimensional reconstruction of human carotid arteries from images obtained during non-invasive B-mode ultrasound examination", *The American Journal of Cardiology*, 70, 379–384, August 1992.

[2] M. G. Bond, S.K. Wilmoth, et alii, "Detection and Monitoring of Asymptomatic Atherosclerosisi in Clinical Trials", *The Americal Journal of Medicine*, vol. 86, (suppl 4A), pp. 33-36, 1989.

[3] J.E. Wilhjelm, et alii, "Estimation of plaque contents with multi-angle 3D compound imaging", *Proc. Of IEEE Ultrasonic Symp.*, pp. 1077-1080, 1996.

[4] J. D. Gill, H. M. Ladak, D.A. Steinman, A. Fenster, " Segmentation of ulcerated plaque: a semi-automatic method for tracking the progression of carotid atherosclerosis", *Proc. of EMBS Conf.*, pp. 669-672, 2000.

[5] J. A. Hossack, T.S. Sumanaweera, S. Napel, "Quantitative 3D ultrasound imaging using an automated image tracking technique", *Proc. Of IEEE Ultrasonic symposium*, pp. 1593-1596, 2000.

[6] C. Liguori, A. Paolillo, A. Pietrosanto, "An automatic measurement system for the evaluation of carotid intima-media thickness", *IEEE Trans. on I&M*, vol. 50 N.6, pp. 1684-1691, Dec. 2001.

[7] A. Fenster, D. B. Downey, "3-D ultrasound imaging: A review", IEEE Engineering in Medicine and Biology, 15, pp. 41–51, 11 1996.

[8] Q. Liang, I. Wendelhag, J. Wikstrand, T. Gustavsson, "A Dynamic Multiscale Programming Procedure for Boundary Detection in Ultrasonic Artery Images", *IEEE Transactions on Medical Imaging*, Vol.19, No.2, February 2000.

[9] G. Betta, C. Liguori, A. Pietrosanto, "A structured approach to estimate the measurement uncertainty in digital signal processing algorithms", *Proc. Inst. Elect. Eng. Sci. Meas. Technol*, vol. 146, pp.21-26, 1999.

[10] "Guide to the expression of uncertainty in measurement (GUM)", *Int. Stand. Org. (ISO)*, 1999.